

Chapman University

Chapman University Digital Commons

Pharmacy Faculty Articles and Research

School of Pharmacy

11-5-2018


Kinetics of Dextromethorphan-O-Demethylase Activity and Distribution of CYP2D in Four Commonly-Used Subcellular Fractions of Rat Brain

Barent N. Dubois

Farideh Amirrad

Reza Mehvar

Follow this and additional works at: https://digitalcommons.chapman.edu/pharmacy_articles

 Part of the [Animals Commons](#), [Chemical and Pharmacologic Phenomena Commons](#), [Enzymes and Coenzymes Commons](#), [Genetic Phenomena Commons](#), [Genetic Structures Commons](#), [Medical Biochemistry Commons](#), [Medicinal and Pharmaceutical Chemistry Commons](#), [Nervous System Commons](#), and the [Other Pharmacy and Pharmaceutical Sciences Commons](#)

Kinetics of dextromethorphan-O-demethylase activity and distribution of CYP2D in four commonly-used subcellular fractions of rat brain

Barent N. DuBois, Farideh Amirrad, and Reza Mehvar

Department of Biomedical and Pharmaceutical Sciences, School of Pharmacy, Chapman University, Irvine, CA, USA

Kinetics of dextromethorphan-O-demethylase activity and distribution of CYP2D in four commonly-used subcellular fractions of rat brain

Abstract

1. The purpose of this study was to compare the enzymatic kinetics and distribution of cytochrome P450 2D (CYP2D) among different rat brain subcellular fractions.
2. Rat brains were used to prepare total membrane, crude mitochondrial, purified mitochondrial, and microsomal fractions, in addition to total homogenate. Michaelis-Menten kinetics of the brain CYP2D activity was estimated based on the conversion of dextromethorphan (DXM) to dextrorphan using UPLC-MS/MS. Protein levels of CYP2D and subcellular markers were determined by Western blot.
3. Microsomal CYP2D exhibited high affinity and low capacity, compared with the mitochondrial CYP2D that had a much lower (~ 50-fold) affinity but a higher (~six-fold) capacity. The apparent CYP2D affinity and capacity of the crude mitochondria were in between those of the microsomes and purified mitochondria. Additionally, the CYP2D activity in the whole homogenate was much higher than that in the total membranes at higher DXM concentrations. A CYP2D immune-reactive band in the brain mitochondria appeared at a lower MW but had a much higher intensity than that in the microsomes.
4. Mitochondrial brain CYP2D has a much higher capacity than its microsomal counterpart. Additionally, brain homogenate is more representative of the overall CYP2D activity than the widely-used total membrane fraction.

Keywords: CYP2D; drug metabolism; rat brain; microsomes; mitochondria; dextromethorphan; dextromethorphan-O-demethylase activity; Michaelis-Menten kinetics

Introduction

Cytochrome P450 (CYP450) 2D6 (CYP2D6) is an isoform of the CYP450 superfamily of drug metabolizing enzymes, which is responsible for the metabolism of many centrally-acting drugs and neurotransmitters (McMillan & Tyndale, 2018; Miksys & Tyndale, 2002; Navarro-Mabarak et al., 2018; Sangar et al., 2009; Wang et al., 2014). The rat CYP2D subfamily shares homology with human CYP2D6, resulting in significant overlap in substrate specificity amongst rat CYP2D1-5 isoforms and human CYP2D6 (Hiroi et al., 2002; Miksys et al., 2000; Tyndale et al., 1999). While mRNA studies have shown that CYP2D4 is the predominant isoform in the rat brain (Funae et al., 2003; Hiroi et al., 1998), other isoforms of CYP2D, such as 2D1 or 2D5, have also been detected in the rat brain, albeit at much lower concentrations (Miksys et al., 2000; Mizuno et al., 2003; Wyss et al., 1995). Studies with rats and monkeys have shown that the concentration and pharmacological response of analgesics and antipsychotics are better correlated with the variability in CYP2D enzyme activity in the brain, as opposed to the hepatic CYP2D (McMillan & Tyndale, 2015; Wang et al., 2015; Zhou et al., 2013). Additionally, induction of brain CYP2D can be independent of its expression in the liver (Mann et al., 2008; Yue et al., 2008). The genomic variation in CYP2D6 in humans has been correlated with behavioral and psychopathological patterns and is speculated to be related to CYP2D's involvement in the biotransformation of serotonin and dopamine (Penas-Lledo & Llerena, 2014). Therefore, investigation of the brain CYP2D expression and activity is crucial to our understanding of the effects of centrally-acting drugs and diseases associated with the changes in the synthesis of neurotransmitters.

Mechanistic studies of CYP450 in brain are more complicated than those in the liver, which is the major organ for CYP450-mediated drug metabolism. This is due to the overall low concentrations of CYP450 enzymes, such as CYP2D, in the brain, which makes quantification of

their metabolic activities difficult (Toselli et al., 2016). Additionally, there is heterogeneity in the expression of CYP2D within the cells and between different regions of the brain (McMillan & Tyndale, 2018; Toselli et al., 2016). To overcome these obstacles, many studies have pooled brains from several rodents to obtain enough tissue for characterization of CYP2D activity (Asai et al., 2018; Coleman et al., 2000; Jolivalt et al., 1995; Voirol et al., 2000). Others (Mann et al., 2008; Toselli et al., 2016; Yue et al., 2008) have relied on methods like RT-PCR and/or Western blotting, instead of enzymatic activity, to estimate changes in the brain CYP2D status. Those studies that have successfully measured functional activity of brain CYP2D utilizing probe substrates, such as dextromethorphan (DXM), tend to either focus on microsomal activity (Asai et al., 2018; Coleman et al., 2000; Jolivalt et al., 1995; Voirol et al., 2000) or something called a “total membrane” fraction (McMillan & Tyndale, 2017; Miksys et al., 2017; Tyndale et al., 1999; Zhou et al., 2013), which is a pooling of all membranes, including microsomes and mitochondria.

Although brain CYP2D is expressed in both endoplasmic reticulum (i.e., microsomes) and mitochondria (Miksys et al., 2000; Tyndale et al., 1999), it should not be assumed that its functionality in a total membrane fraction would be an accurate reflection of that in the individual subcellular fractions or the entire cell. This is because CYP450 enzymes in different subcellular compartments utilize different reductases for transferring electrons from NADPH (Anandatheerthavarada et al., 1997; Boopathi et al., 2000; Dasari et al., 2006), which may or may not be available to the same extent in the total membrane fraction. Therefore, the information obtained from the studies of CYP2D activity in the total membrane fractions may not be easily extrapolated to the activity of this enzyme in the cell.

Despite recognition of the presence of CYP2D in the brain mitochondria (Miksys et al., 2000; Tyndale et al., 1999), a complete characterization of mitochondrial CYP2D activity,

including its Michaelis-Menten (MM) kinetics are absent from the literature. Furthermore, we are not aware of any comparison of the kinetics of CYP2D activity among commonly-used subcellular fractions in the same brain sample. Therefore, the major aim of this study was to determine the kinetics of DXM demethylation in the rat brain microsomal, mitochondrial, and total membrane fractions in a side-by-side comparison. Considering mitochondria can vary in purity, we also compared Percoll-gradient purified mitochondria to unpurified “crude” mitochondria. Further, the kinetics of CYP2D activity was investigated in the whole brain homogenate as a potential alternative to the total membrane fraction. In addition to the kinetic studies of the enzymatic activity, we also measured the protein content of CYP2D in different subcellular fractions using Western blot analysis to determine if any correlations exist between enzymatic activity and CYP2D content.

Methods

Chemicals and antibodies

Dextromethorphan (DXM) was purchased from United States Pharmacopeial Convention (Rockville, MD, USA). Analytical metabolite standard solutions for dextrophan tartrate (DXT) and its stable isotope d_3 -dextrophan were purchased from Cerilliant Corporation (Round Rock, TX, USA). Primary antibodies raised in rabbit against CYP2D1 (ab22590), calreticulin (ab92516), and voltage-dependent anion-selective channel 1 (VDAC1)/Porin (ab15895) were purchased from Abcam (Cambridge, MA, USA). Although the CYP2D1 antibody is raised against CYP2D1, it should be noted that because of significant homology (77% to 83%) among rat CYP2D isoforms 1-5 (Funae et al., 2003), it is very likely that the antibody reacts with other rat CYP2D isoforms as well. The fluorescent secondary antibody Donkey Anti-Rabbit IgG H&L (Alexa Fluor® 680) and

HRP-conjugated Goat Anti-Rabbit IgG H&L were purchased from Abcam. All other reagents and chemicals were analytical grade and purchased from commercial sources.

Preparation of subcellular fractions from whole rat brain

Although separate protocols are reported in the literature for preparation of brain total membrane (Miksys et al., 2000), crude and purified mitochondrial (Kristian, 2010), and microsomal (Bhagwat et al., 1995; Jolivald et al., 1995; Voirol et al., 2000) fractions, to the best of our knowledge, there is no single protocol for preparation of all the fractions from the same brain tissue. Thus, the protocols from these different studies were adapted into a single procedure to generate all four fractions, which necessitated some modifications to the homogenization and storage buffer compositions, as described below.

Frozen whole brains from adult (8 to 12-week old), male Sprague-Dawley rats were purchased from Innovative Research (Novi, Michigan, USA). Pooled whole brains (2 brains per preparation) were homogenized in ice-cold buffer (100 mM Tris, 0.2 mM EDTA, and 1.15% KCl; pH 7.4) at a 1:10 ratio using an electric motor-driven Potter-Elvehjem Teflon homogenizer. The homogenate was divided into two tubes. One tube was used to generate the crude mitochondrial (CM) and total membrane (TM) fractions. The other tube was used for collection of purified mitochondria (PM) and microsomes (MC). Each homogenate tube was first spun at 1300 g for 5 minutes at 4°C. The supernatant was collected, and the pellet washed with the homogenizing buffer and centrifuged again at 1300 g for 5 minutes. For each tube, the original and wash supernatants were combined and used for the preparation of the individual fractions as described below. A total of 5 preparations were made from 5 different brain pools, with 4 fractions per preparation.

The collected pellets from each respective fraction, prepared as described below, were re-suspended in storage buffer (100 mM Tris, 0.2 mM EDTA, 1.15% KCl, 20% glycerol, 0.1 mM dithiothreitol, 22 µM butylated hydroxytoluene, and 0.1 mM phenylmethylsulfonyl fluoride; pH

7.4) (Bhagwat et al., 1995) and stored at -80°C for later experiments. Total protein concentrations were estimated using the Bradford method.

Total membranes (TM)

The 1300-g supernatant was spun at 110,000 g for 70 minutes at 4°C. The supernatant was discarded, and the pellet was washed and centrifuged again using fresh homogenization buffer. The TM pellet was then collected and re-suspended in the storage buffer.

Crude mitochondria (CM)

The 1300-g supernatant was spun at 21,000 g for 12 minutes at 4°C. The supernatant was discarded and the pellet was washed and centrifuged again using fresh homogenization buffer. The CM pellet was collected and re-suspended in the storage buffer.

Purified mitochondria (PM)

The crude mitochondrial pellet was generated as described above. The pellet was re-suspended in the homogenization buffer with 15% Percoll and run twice on a 15%/24%/40% Percoll gradient, which was spun at 30,700 g for 12 minutes at minimal acceleration and no brakes. The layer containing PM, at the interface between the 24% and 40% Percoll layers, was collected and washed 3 to 4 times, with the homogenization buffer by spinning at 21,000 g. The final non-synaptic PM pellet was re-suspended in the storage buffer.

Microsomes (MC)

The 1300-g supernatant was spun at 21,000 g for 12 minutes at 4°C. The supernatant was collected and spun at 110,000 g for 70 minutes. The pellet was washed and centrifuged again using fresh homogenization buffer. The MC pellet was collected and re-suspended in the storage buffer.

Preparation of whole homogenate (WH)

In addition to the four individual fractions above, we also prepared WH from additional 5 rat brains in a separate experiment. Individual, frozen rat brains were homogenized at a 1:10 ratio in the homogenization buffer as described above and stored at -80°C.

Dextromethorphan O-demethylase activity

The assay for dextromethorphan O-demethylase (DOD) activity was carried out in a 100 mM Tris-HCl buffer (pH 7.4) and a protein concentration of 0.2 mg/mL. For these assays, DXM stock solutions were prepared by dissolving the powder in 5 mM excess HCl solutions. For MC and TM fractions, DXM concentrations were 100, 200, 500, 1000, 1500, and 2000 μ M, whereas the activity in WH, CM, and PM was measured at substrate concentrations of 100, 200, 500, 1000, 2000, 5000, and 10000 μ M. The reaction mixtures (25 μ L) contained buffer, sample protein, and substrate. After 5 minutes preincubation at 37°C, the reaction was initiated by the addition of 1 mM NADPH. After 20 minutes incubation at 37°C, reactions were terminated by the addition of ice-cold acetonitrile (75 μ L), containing internal standard. Each reaction mixture was paired with its own control sample (time zero), containing all the elements of the reaction mixture with the exception of NADPH. The reactions in the control samples were immediately terminated by the addition of ice-cold acetonitrile containing internal standard. Samples were centrifuged, and the supernatant was used for LC-MS/MS analysis.

UPLC-MS/MS analysis of dextromethorphan metabolite

The sample preparation for the analysis of DXT consisted of precipitation of proteins in the reaction mixture (25 μ L) by the addition of 75 μ L of ice-cold acetonitrile, containing 10 nM internal standard (d_3 -dextrophan). Samples were then vortexed, centrifuged at 13,400 rpm for 5 minutes, and the supernatant collected for the LC-MS/MS analysis.

The concentrations of DXT in the subcellular fractions were quantitated using a validated UPLC-MS/MS method (DuBois & Mehvar, 2018). Briefly, the UPLC-MS/MS system consisted of a Kinetex 1.7 μm C18 (100 A, 100 x 2.1 mm) column (Phenomenex; Torrance, CA, USA), connected to a Bruker (Billerica, MA, USA) EVOQ triple quadrupole mass spectrometer. Samples (2 μL) were injected onto the column and eluted at a flow rate of 0.2 mL/min at 40°C under gradient conditions with 5 mM ammonium formate and 0.05% formic acid in water (A) and 95% acetonitrile, 5% methanol, and 0.05% formic acid (B). Gradient conditions were as follows: 0-0.5 minutes, 10% B; 0.5-4 min, linear gradient 10-90% B; 4-7 min, 90% B; 7 min, 10% B; 7-9 min, 10% B. Retention time for DXT and its stable isotope was 2.75 minutes. The source utilized heated electrospray ionization (needle temperature 300°C, flow 40 psi; cone temperature 300°C, flow 20 psi; nebulizer gas flow 50 psi) in positive ion mode at 3000 V. Metabolite and internal standard were analyzed using selected reaction monitoring for the parent/fragment transitions of m/z 258 \rightarrow 156.90 for DXT and m/z 261 \rightarrow 156.90 for d_3 -DXT. The standard curve for DXT was linear between 0.25 to 100 nM ($r^2 \geq 0.99$) with lower limit of quantitation of 0.25 nM and inter- and intra-day accuracies between 94.1 to 111% and precision (relative standard deviation) values of $\leq 14.9\%$.

Immunoblotting experiments

Proteins (3-15 μg) from subcellular fractions were subjected to SDS-polyacrylamide gel electrophoresis on a precast Bio-Rad (Hercules, CA, USA) 4-20% MP TGX Stain-Free gels for CYP2D1 or 12% MP TGX gels for calreticulin and VDAC at constant voltage (200 V) for 30 minutes. Proteins were transferred with the Bio-Rad Trans-Blot Turbo Transfer System onto 0.45 μm (CYP2D1) or 0.20 μm (calreticulin and VDAC) PVDF membranes. Membranes were blocked with 3% blotting grade, non-fat milk (CYP2D1) or 5% BSA (calreticulin and VDAC) for 1 hour at room temperature, then incubated overnight with primary antibody for CYP2D1 (1:1,000),

calreticulin (1:10,000), or VDAC (1:50,000). After washing, membranes were incubated with fluorescent (CYP2D, 1:5,000) or HRP-conjugated (calreticulin and VDAC, 1:50,000) secondary antibodies for 1 hour at room temperature, then washed before visualization of bands with the Bio-Rad ChemiDoc Imager system.

Data analysis

Because of presence of some impurities of DXT in the DXM stock solution (DuBois & Mehvar, 2018), the rate of production of the metabolite was corrected by subtracting the amount of metabolite in the control sample (time zero) from that in the sample after 20 min of incubation. The metabolism rate-substrate concentration profile for each subcellular fraction was fitted to the following three models.

Single-enzyme, MM model

This model fits the DOD rate (V)-substrate concentration (S) data to a single-enzyme system with MM parameters of maximum velocity (V_{max}) and MM constant (K_m):

$$V = \frac{V_{max} \times S}{K_m + S} \quad (1)$$

Two-enzyme, MM model

This model fits the DOD rate-substrate concentration data to a two-enzyme system with MM parameters of V_{max1} and K_{m1} for the first enzyme and V_{max2} and K_{m2} for the second enzyme:

$$V = \frac{V_{max1} \times S}{K_{m1} + S} + \times \frac{V_{max2} \times S}{K_{m2} + S} \quad (2)$$

Two-enzyme, mixed model

This model uses a two-enzyme system, one with a MM behavior with parameters of V_{max1} and K_{m1} and the other with a linear behavior within the studied substrate range with an intrinsic clearance of CL_{int2} :

$$V = \frac{V_{max1} \times S}{K_{m1} + S} + (CL_{int2} \times S) \quad (3)$$

The best fit model describing the experimental data for each subcellular fraction was selected based on the evaluation of Eadie-Hofstee transformed plots and the Akaike's Information Criterion (AIC). Additionally, the intrinsic clearance (CL_{int}) for each enzyme system with MM characteristics was calculated by dividing V_{max} by K_m of the enzyme.

Statistical analyses were performed with repeated measure, one-way ANOVA, followed by Tukey's post-hoc test, or with unpaired, two-tailed t-tests. A p value of < 0.05 was considered significant. Data are presented as mean \pm SD. Statistical and nonlinear regression analyses were performed with GraphPad Prism (v7.04) software (La Jolla, CA, USA).

Results

Dextromethorphan O-demethylase activity in subcellular fractions

Figure 1A depicts the kinetics of DOD activity in the microsomal (MC), crude mitochondrial (CM), and purified mitochondrial (PM) fractions. Based on both Eadie-Hofstee plots and AIC (data not shown), all the individual microsomal (MC) and purified mitochondrial (PM) fractions were best described by the single-enzyme, MM model. Similar to the MC and PM fractions, AIC also suggested the single-enzyme model as the best fit model for the crude mitochondrial (CM) samples. However, the Eadie-Hofstee plots were more ambiguous as some CM samples showed signs of nonlinearity, which is an indication of presence of multiple enzymes. Nevertheless, because of lack of sufficient number of data points to accurately estimate the parameters of a multi-enzyme system, we used the simpler single-enzyme model for the description of CM fraction data as well. In microsomes, the metabolic rate plateaued between substrate concentrations of 1000 and 2000 μ M (Fig. 1A). In contrast to the microsomes, the DOD activity of the crude and purified mitochondrial fractions did not reach a clear plateau, even at substrate concentrations as high as

10,000 μM (Fig. 1A), which was the limit of solubility of substrate in our reactions. However, at substrate concentrations ≤ 2000 μM , the crude and purified mitochondrial fractions exhibited lower DOD activities relative to microsomes (Fig. 1A).

The activity-substrate concentration profiles in the whole homogenate (WH) and total membrane (TM) fraction, which were best fit to the two-enzyme, mixed model (based on both Eadie-Hofstee plots and AIC), are shown in Fig. 1B. Whereas at substrate concentrations below 2000 μM , the relationship between the observed activity and substrate concentration was nonlinear, there was an almost linear relationships between the two parameters at concentrations between 2000 to 10000 μM (Fig 1B).

Figure 2 depicts the single-enzyme, MM parameters V_{max} (Fig. 2A), K_m (Fig. 2B), and CL_{int} (Fig. 2C) for the brain microsomal (MC), crude mitochondrial (CM), and purified mitochondrial (PM) fractions. The estimated V_{max} value (pmol/min/mg protein) for microsomes (3.40 ± 0.28) was significantly ($p < 0.05$) lower than the corresponding values for the crude (8.35 ± 1.87) or purified (19.4 ± 3.4) mitochondria (Fig. 2A). Indeed, the relatively high V_{max} values for both mitochondrial fractions were outside the observed experimental range of tested substrate concentrations (Fig. 1A). However, purified mitochondria had a significantly higher V_{max} , compared with the crude mitochondria (Fig. 2A). Similarly, the K_m values (μM) for the microsomes (220 ± 24) were significantly lower than the values for the crude (6680 ± 2500) or purified ($10,500 \pm 2320$) mitochondria (Fig. 2B). Among all the fractions, purified mitochondria had the highest apparent K_m , but this was not significantly different from the value in the crude mitochondria (Fig. 2B). As for the apparent CL_{int} ($\mu\text{L/hr/mg}$), microsomes showed by far the highest ($p < 0.001$) value (0.937 ± 0.149), when compared with the values in the crude ($0.0776 \pm$

0.0096) or purified (0.114 ± 0.030) mitochondria (Fig. 2C). However, there was no significant difference in the CL_{int} values between the crude and purified mitochondria.

Figure 3 depicts the parameters of the two-enzyme, mixed model, which was the best fit to the total membrane (TM) fraction and whole homogenate (WH) data. For the first enzyme, the estimated parameters (V_{max1} , K_{m1} , and CL_{int1}) in the TM fraction were not significantly different from those in the WH (Figs. 3A, 3B, and 3C). However, for the second enzyme, there was a significant difference ($p < 0.0001$) between TM and WH in their CL_{int2} values ($\mu\text{L}\cdot\text{hr}^{-1}\cdot\text{mg}^{-1}$), which were 2.4-fold higher in WH (0.0413 ± 0.004) than those in TM (0.0173 ± 0.003).

Subcellular localization of CYP2D and marker proteins CPR and VDAC

The Western blot data for CYP2D, VDAC, and calreticulin are presented in Figure 4. For CYP2D, an immune-reactive band was observed in the brain microsomes (MC), which corresponded to the same MW (~ 50 kDa) of the positive liver microsomal control (Fig. 4A, right panel). Additionally, a less intense band was present at a lower MW in both the liver and brain MC (Fig. 4A, right panel). In the total membranes (TM), crude mitochondria (CM), and purified mitochondria (PM), an intense immune-reactive band was observed, which corresponded to the lower MW band in MC (Fig. 4A, right panel). Because PM had the highest protein-corrected band intensity, the protein-corrected band intensities are presented as a percentage of the intensity in PM. The CYP2D band intensities in the four brain fractions were in the following order: PM ($100\% \pm 21\%$) $>$ CM ($33.8\% \pm 4.7\%$) = TM ($33.6\% \pm 4.9\%$) $>$ MC ($5.3\% \pm 1.9\%$, higher MW band) (Fig. 4A, left panel). The protein-corrected band intensity in PM was significantly higher than that in all the other fractions ($p < 0.001$). The protein-corrected band intensities in CM and TM were not significantly different from each other but were both significantly greater than the intensity of the higher MW band in MC ($p < 0.01$).

As expected, VDAC, an outer-membrane mitochondrial marker protein with a MW of ~31 kDa, was abundantly present in the brain mitochondrial fractions (Fig. 4B, right panel). Because PM had the highest band intensity, the band intensities are presented as a percentage of intensity in PM. The VDAC intensities in the four brain fractions were in the following order: PM ($100\% \pm 36\%$) > CM ($41.2\% \pm 8.2\%$) > TM ($26.4\% \pm 1.3\%$) > MC ($2.1\% \pm 0.6\%$) (Fig. 4B, left panel). The VDAC intensities in all the four fractions were significantly different from each other (Fig. 4B, left panel).

As expected, calreticulin, an endoplasmic reticulum marker protein, was abundantly present in the brain MC and corresponded to the same MW (~75 kDa) of the positive liver microsomal control sample (Fig. 4C, right panel). Because MC had the highest band intensity, the band intensities of calreticulin are presented as a percentage of intensity in the brain MC. The calreticulin intensities in the four brain fractions were in the following order: MC ($100\% \pm 14.8\%$) > TM ($63.5\% \pm 14.2\%$) > CM ($42.2\% \pm 10.3\%$) > PM ($15.7\% \pm 5.6\%$) (Fig. 4C, left panel). The calreticulin intensities in all the four fractions were significantly different from each other (Fig. 4C, left panel).

Discussion

The recent evidence about the therapeutic and pathophysiologic relevance of brain CYP2D calls for a new evaluation of this enzyme's metabolic behavior related to its subcellular distribution. Despite presence of significant quantities of this enzyme in mitochondria (Miksys et al., 2000; Tyndale et al., 1999), the kinetics of the enzymatic activity of brain CYP2D in mitochondria have not been characterized. Estimating these kinetic parameters would be useful in determining the contribution of these subcellular compartments (endoplasmic reticulum or mitochondria) to the CYP2D-mediated biotransformation of drugs and endogenous compounds in the brain. Therefore,

the main goal of our study was to compare the brain CYP2D metabolic kinetics side-by-side between the endoplasmic reticulum (microsomes) and mitochondria utilizing the DOD activity assay. Our findings suggest that the kinetics of CYP2D-mediated enzymatic activity in the brain are dramatically different between these two subcellular fractions (Figs. 1 and 2). Microsomes exhibited a high affinity (low apparent K_m), low capacity (low apparent V_{max}) metabolic activity, whereas purified mitochondria had a low affinity (high apparent K_m), but a very high capacity (high apparent V_{max}). The finding of a high capacity CYP2D activity in the brain mitochondria is novel, which may have therapeutic, pathophysiologic, and/or toxicologic relevance due to contribution of brain CYP2D to the metabolism of centrally-acting drugs and synthesis of neurotransmitters.

Abundance and activity of CYP2D in brain microsomes and mitochondria

Our immunoblot studies with the CYP2D antibody showed different patterns in the brain microsomal and mitochondrial fractions (Fig. 4A). Whereas the microsomal fraction showed an intense band at a higher MW and a much less intense band at a lower MW, the mitochondrial fractions showed a very intense band at the lower MW (Fig. 4A, right panel). Interestingly, the profile for the control liver microsomal sample was similar to that for the brain microsomes (Fig. 4 A, right panel). It has been reported that CYP2D antibodies cannot reliably distinguish among isozymes within the rat CYP2D subfamily (CYP2D1-5), which have subtle variations in their molecular weights (Miksys et al., 2000). Therefore, it is possible that different CYP2D isoforms, with different MWs, are present in the rat brain mitochondria and microsomes.

Based on mRNA studies, the major CYP2D isoform in the rat brain is CYP2D4 (Funae et al., 2003; Hiroi et al., 1998; Wyss et al., 1995). Additionally, CYP2D1/5 mRNA has also been found in the rat brain although at much lower abundance (Miksys et al., 2000; Mizuno et al., 2003;

Wyss et al., 1995). It has been reported (Miksys et al., 2000) that among the CYP2D isoforms, the MW of CYP2D4 is the lowest. Because CYP2D4 protein is low or absent in the liver (Hiroi et al., 1998), it is likely that the lower band in the liver microsomes (lower MW), which is much less intense than the upper band, is related to CYP2D4 and the more intense upper band (higher MW) is related to CYP2D isoforms other than CYP2D4. Similarly, whereas the more intense upper band in the brain microsomes may be a reflection of CYP2D isoforms other than 2D4, the intense band with the lower MW in the PM may be related to CYP2D4. This hypothesis is in agreement with the significant abundance of the lower band (potentially related to CYP2D4) in the total membrane fraction of rat brain, observed in our studies (Fig. 4A, right panel) and the reported (Funae et al., 2003; Hiroi et al., 1998; Wyss et al., 1995) prominence of CYP2D4 mRNA in the rat brain. However, more specific antibodies are needed to confirm this hypothesis.

In addition to having a lower MW, the CYP2D band in the mitochondrial samples was much more abundant than the major CYP2D band in the microsomes (Fig. 4A). Indeed, the protein-corrected intensity of the CYP2D band in the microsomes (upper band) was ~5% of that in the purified mitochondria. Therefore, the higher apparent V_{\max} in the brain mitochondria relative to microsomes (Fig. 2A) is consistent with the high abundance of CYP2D in mitochondria (Fig. 4A). In fact, the capacity of this enzyme in the pure mitochondrial fraction was difficult to saturate even at substrate concentrations of 10,000 μM (Fig. 1A). These observations are consistent with the initial and oft-cited studies of CYP450 in the brain, which observed several-fold greater amounts of CYP450 in mitochondria (Bhagwat et al., 2000; Ghersi-Egea et al., 1993; Ghersi-Egea et al., 1987). Furthermore, Miksys et al. (Miksys et al., 2000) also showed presence of intense immunoreactive bands in both mitochondrial and microsomal fractions prepared from the rat brains. However, in their studies, the lower band was much more intense than the upper band not

only for mitochondria, but also for microsomes. Although this is consistent with our data for the mitochondria, our CYP2D1 antibody reactive bands in the microsomes showed higher intensity for the upper band (Fig. 4A). Differences in the electrophoresis conditions and selectivity of antibodies towards different CYP2D isoenzymes might have been responsible for the apparent differences between our Western blot data (Fig. 4A) and those of Miksys et al. (Miksys et al., 2000).

Despite high capacity, the mitochondrial DOD activity exhibited a low affinity relative to the microsomes (Fig. 2B) such that the apparent intrinsic clearance (V_{\max}/K_m) in purified mitochondria was almost 9 times lower than that in the microsomes (Fig. 2C). Although studies have observed overall higher CYP450 content in mitochondria (Bhagwat et al., 2000; Ghersi-Egea et al., 1993; Ghersi-Egea et al., 1987), these same studies have also observed either similar or lower activities relative to microsomes. Voirol et al. (Voirol et al., 2000) reported that the DOD activity in the rat brain mitochondria was much lower than that in the microsomes. However, they used substrate concentrations up to 600 μM DXM. This is consistent with our results at substrate concentrations below 2000 μM (Fig. 1A). However, our DOD kinetic studies clearly show for the first time that at higher substrate concentrations, enzymatic activity of the purified mitochondrial fraction is several-fold higher than that of the microsomal fraction (Fig. 1A).

In addition to the possibility of the presence of a different CYP2D isoform in the mitochondria, other factors may have also contributed to the apparent lower affinity of mitochondrial CYP2D observed in our study. For instance, post-translational modification of CYP2D for targeting to the mitochondria (Anandatheerthavarada et al., 1999; Boopathi et al., 2000; Dasari et al., 2006) may affect its affinity. Another contributing factor to the lower affinity in the mitochondria might be related to the major differences between the mitochondria and

microsomes in their CYP450 electron transferring mechanisms. In the microsomes, cytochrome P450 reductase (CPR) is responsible for the electron transfer to CYP450, and both CYP450 and CPR are integrally membrane-bound proteins. However, the electron transfer system in mitochondria consists of two soluble proteins, adrenodoxin (Adx) and adrenodoxin reductase (Adr), which are present in the inner membrane matrix. During the preparation of mitochondrial fractions, it is possible that the inner and/or outer membranes of some mitochondria are disrupted, resulting in a reduction in the concentrations of Adx and Adr proteins in the mitochondrial matrix (Dasari et al., 2006; Sangar et al., 2009). Consequently, the apparently low affinity (Fig. 2B) and intrinsic clearance (Fig. 2C) of the CYP2D-mediated DOD in mitochondria, compared with the respective values in the microsomes, could be partially related to some loss of Adx and Adr during the preparation of mitochondria.

Subcellular fraction purity

Because of the nature of differential centrifugation, there is always some degree of contamination of various subcellular fractions prepared by this method. Therefore, we used VDAC, a mitochondrial marker, to determine the contamination of microsomes by mitochondria, and calreticulin, a microsomal marker, to estimate the degree of contamination of purified mitochondria by microsomes. As the data in Fig. 4B indicate, the degree of contamination of microsomes with mitochondria, based on VDAC presence, was negligible (~ 2%). Additionally, the degree of contamination of Percoll-purified mitochondrial fraction with microsomes, based on calreticulin presence, was ~16% (Fig. 4C). These data suggest that the enzymatic activities (Figs. 1 and 2) and CYP2D band intensities (Fig. 4A) in the microsomal and Percoll-purified mitochondrial fractions are relatively accurate measures for these two fractions.

Because crude, instead of purified, mitochondria is commonly used in brain CYP450 studies (Gherssi-Egea et al., 1993; Lavandera et al., 2015; Miksys et al., 2000; Voirol et al., 2000), we also investigated the CYP2D activity and expression in this fraction. As expected, the crude mitochondrial fraction had a higher degree of microsomal contamination (42%) than the Percoll-purified mitochondria (16%), based on calreticulin (Fig. 4C). This microsomal contamination could explain the significantly lower V_{\max} and K_m values (Figs. 1 and 2) and band intensity (Fig. 4A) for the crude mitochondria relative to those for the purified mitochondria. These data suggest that studies that use crude mitochondrial fraction may not accurately reflect the true metabolic characteristics of the mitochondrial CYP2D in the brain.

Despite presence of 42% microsomal impurity, the CM fraction only showed one band at the lower MW, corresponding to that in the PM fraction (Fig. 4A, right panel). The lack of a visible upper microsomal band in the CM fraction might be explained by the fact that the upper band in the MC fraction was equivalent to only 5% of the CYP2D band in the pure mitochondria (See *Abundance and activity of CYP2D in brain microsomes and mitochondria*). Therefore, in the presence of substantial mitochondrial band in the CM fraction, the upper band related to the microsomal impurity may not be easily visible.

The total membrane fraction versus brain homogenate

Many studies of the brain CYP450 isoforms have used a total membrane fraction as an overall measure of the brain activity/content (Agarwal et al., 2008; Mann et al., 2008; McMillan & Tyndale, 2015; Miksys et al., 2000; Miksys et al., 2017; Tyndale et al., 1999; Wu et al., 2011). This is because the total membrane fraction would contain all the functional cellular CYP450, which are membrane bound proteins. However, it is not known how the total membrane fraction would compare with the whole brain homogenate, which is easily and quickly prepared without

any ultracentrifugation process. Because of the presence of several DXM-metabolizing subcellular compartments in both TM and WH, a simple, one-enzyme system could not fit the data for these preparations. Instead, a two-enzyme, mixed model with an apparent MM kinetics, to describe the early phase (lower DXM concentrations), and an apparent linear model, to describe the late phase (higher DXM concentration), was necessary (Fig. 1B).

Our data with the MC and PM fractions (Fig. 1A) suggest that whereas the kinetic profiles of TM and WH at lower DXM concentrations are mostly influenced by its microsomal content, the mitochondrial fraction would likely dominate the profiles at the higher DXM concentrations (Fig. 1B). Therefore, similarity of the TM and WH profiles at lower DXM concentration (Fig. 1B), associated with the similar MM parameters for the first enzyme (Fig. 3), suggest that the contribution of microsomes to the metabolism of DXM is similar in TM and WH. However, the lower CYP2D activity in the TM fraction, compared to that in WH, at high substrate concentrations (Fig. 1B), along with the significantly lower Cl_{int2} value in TM (Fig. 3D), suggests that the mitochondrial membranes present in the TM fraction are less active than the mitochondrial structures present in WH.

The differences between TM and WH in their DOD activity might be related to the extent of availability of the electron-donating systems in these preparations. Whereas the membrane-bound microsomal CPR is expected to be fully present in both TM and WH, the soluble mitochondrial Adx and Adr may be lower or absent in the TM fraction because of the centrifugation process and shear stress (Wattiaux-De Coninck et al., 1974). Therefore, the mitochondrial CYP2D in TM might be less active than its counterpart in WH. Collectively, our data suggest that the whole brain homogenate might be superior to total membrane fractions as an

overall measure of the metabolic activity of CYP2D, and potentially other CYP450 isoforms, in the rat brain.

Although we are not aware of any other study reporting the kinetics of DOD activity in the rat brain homogenate, the kinetics of DOD activity in the rat brain total membrane have been reported before (Tyndale et al., 1999). That study (Tyndale et al., 1999) used a two-enzyme (MM) model to fit the data in a substrate concentrations range of 0.5 to 600 μM . The activity-substrate concentration profile in the study of Tyndale et al. was similar to the profile observed in our study at concentrations below 600 μM (Fig. 1B). Additionally, our estimates for the apparent $V_{\text{max}1}$ and $K_{\text{m}1}$ in the total membrane fraction (Fig. 3) were similar to the high-capacity, low affinity enzyme in their two-enzyme system (Tyndale et al., 1999). However, our study, which included a much higher substrate concentration range of 10,000 μM (as opposed to 600 μM), clearly identified a much higher capacity enzyme. Collectively, these data indicate that the kinetics of DOD activity in the total membrane fraction is very complex, due to presence of membranes and enzymes from several different subcellular compartments and their interactions. Therefore, the models that best fit the data depend on the studied substrate concentration range and may not be a true reflection of available enzymes and their characteristics.

Comparison of DOD activity with CYP2D-mediated metabolism of other substrates

In addition to the available kinetic data on the DOD activity in the rat brain microsomes, a previous study (Coleman et al., 2000) also reported the kinetics of metabolism (1'-hydroxylation) of bufuralol, a known substrate for the human CYP2D6 enzyme, in the rat brain microsomes. The authors showed that the kinetics of bufuralol 1'-hydroxylation in the rat brain microsomes was best described by a two enzyme model, one with MM characteristics and the other with a Hill function. However, the previous studies (Jolivald et al., 1995; Voirol et al., 2000) and our own data (Fig.

1A) suggest a one-enzyme system in the rat brain microsomes when DXM is used as a substrate. These differences could be due to the choice of substrate as well as the concentration ranges studied. Furthermore, it was shown (Coleman et al., 2000; Wan et al., 1997) that different isoforms of rat CYP2D may have different substrate specificity. Studies in yeast cells expressing rat CYP2D1, 2D2, 2D3, and 2D4 showed whereas bufuralol 1'-hydroxylation was similar among the four isoforms, CYP2D2 showed the highest debrisoquin 4-hydroxylation activity and CYP2D3 showed the highest lidocaine N-deethylation activity. We are not aware of any similar data about the specificity or selectivity of different rat CYP2D isoforms towards DOD. Therefore, it remains to be seen whether the kinetic differences in the DOD activity among different brain fractions reported here may be extrapolated to other CYP2D substrates.

Conclusions

A side-by-side comparison of the kinetics of DOD activity in microsomal and purified mitochondrial fractions revealed a novel, high capacity enzyme in the mitochondria with a V_{\max} that is at least six-fold higher than that in the brain microsomes. Additionally, the kinetics of DOD activity in the total membrane and crude mitochondrial fractions, which are commonly used in rat brain studies of CYP2D-mediated metabolism, were dependent on their relative contents of mitochondrial and microsomal compartments and their electron-donating proteins. Further, a comparison of the total membrane fraction with whole homogenate suggests that the latter is a more accurate representative of the overall brain tissue activity of CYP2D. It is concluded that brain fractions containing mixtures of mitochondria and microsomes, such as total membranes, could obfuscate true differences between these subcellular compartments in their CYP2D activities. Further investigations are needed to determine the pharmacological or toxicological relevance of the high capacity brain mitochondrial CYP2D characterized in our studies. Although

mitochondria CYP2D may play a smaller role in the metabolism of therapeutic concentrations of xenobiotics, it may have a more significant role in drug overdoses and/or pathophysiologic conditions affecting mitochondria.

Acknowledgments

This study was supported by funding from XXX University School of Pharmacy, and by the American Liver Foundation's Postdoctoral Research Fellowship Award to XXX.

Declaration of interests

The authors have no conflicts of interest to declare.

References

- Agarwal V, Kommaddi RP, Valli K, Ryder D, Hyde TM, Kleinman JE, Strobel HW, Ravindranath V. (2008). Drug metabolism in human brain: high levels of cytochrome P4503A43 in brain and metabolism of anti-anxiety drug alprazolam to its active metabolite. *PLoS One*, 3: e2337.
- Anandatheerthavarada HK, Addya S, Dwivedi RS, Biswas G, Mullick J, Avadhani NG. (1997). Localization of multiple forms of inducible cytochromes P450 in rat liver mitochondria: immunological characteristics and patterns of xenobiotic substrate metabolism. *Arch Biochem Biophys*, 339: 136-50.
- Anandatheerthavarada HK, Biswas G, Mullick J, Sepuri NB, Otvos L, Pain D, Avadhani NG. (1999). Dual targeting of cytochrome P4502B1 to endoplasmic reticulum and mitochondria involves a novel signal activation by cyclic AMP-dependent phosphorylation at ser128. *EMBO J*, 18: 5494-504.
- Asai Y, Tanaka H, Nadai M, Katoh M. (2018). Status Epilepticus Decreases Brain Cytochrome P450 2D4 Expression in Rats. *J Pharm Sci*, 107: 975-8.
- Bhagwat SV, Boyd MR, Ravindranath V. (1995). Rat brain cytochrome P450. Reassessment of monooxygenase activities and cytochrome P450 levels. *Drug Metab Dispos*, 23: 651-4.
- Bhagwat SV, Boyd MR, Ravindranath V. (2000). Multiple forms of cytochrome P450 and associated monooxygenase activities in human brain mitochondria. *Biochem Pharmacol*, 59: 573-82.
- Boopathi E, Anandatheerthavarada HK, Bhagwat SV, Biswas G, Fang JK, Avadhani NG. (2000). Accumulation of mitochondrial P450MT2, NH(2)-terminal truncated cytochrome P4501A1 in rat brain during chronic treatment with beta-naphthoflavone. A role in the metabolism of neuroactive drugs. *J Biol Chem*, 275: 34415-23.

Coleman T, Spellman EF, Rostami-Hodjegan A, Lennard MS, Tucker GT. (2000). The 1'-hydroxylation of Rac-bufuralol by rat brain microsomes. *Drug Metab Dispos*, 28: 1094-9.

Dasari VR, Anandatheerthavarada HK, Robin MA, Boopathi E, Biswas G, Fang JK, Nebert DW, Avadhani NG. (2006). Role of protein kinase C-mediated protein phosphorylation in mitochondrial translocation of mouse CYP1A1, which contains a non-canonical targeting signal. *J Biol Chem*, 281: 30834-47.

DuBois BN, Mehvar R. (2018). UPLC-MS/MS analysis of dextromethorphan-O-demethylation kinetics in rat brain microsomes. *J Chromatogr B Analyt Technol Biomed Life Sci*, 1096: 66-72.

Funae Y, Kishimoto W, Cho T, Niwa T, Hiroi T. (2003). CYP2D in the brain. *Drug Metab Pharmacokinet*, 18: 337-49.

Gherzi-Egea JF, Perrin R, Leininger-Muller B, Grassiot MC, Jeandel C, Floquet J, Cuny G, Siest G, Minn A. (1993). Subcellular localization of cytochrome P450, and activities of several enzymes responsible for drug metabolism in the human brain. *Biochem Pharmacol*, 45: 647-58.

Gherzi-Egea JF, Walther B, Minn A, Siest G. (1987). Quantitative measurement of cerebral cytochrome P-450 by second derivative spectrophotometry. *J Neurosci Methods*, 20: 261-9.

Hiroi T, Chow T, Imaoka S, Funae Y. (2002). Catalytic specificity of CYP2D isoforms in rat and human. *Drug Metab Dispos*, 30: 970-6.

Hiroi T, Imaoka S, Chow T, Funae Y. (1998). Tissue distributions of CYP2D1, 2D2, 2D3 and 2D4 mRNA in rats detected by RT-PCR. *Biochim Biophys Acta*, 1380: 305-12.

Jolivalt C, Minn A, Vincent-Viry M, Galteau MM, Siest G. (1995). Dextromethorphan O-demethylase activity in rat brain microsomes. *Neurosci Lett*, 187: 65-8.

- Kristian T. (2010). Isolation of mitochondria from the CNS. *Curr Protoc Neurosci*, Chapter 7: Unit 7 22.
- Lavandera J, Ruspini S, Batlle A, Buzaleh AM. (2015). Cytochrome P450 expression in mouse brain: specific isoenzymes involved in Phase I metabolizing system of porphyrinogenic agents in both microsomes and mitochondria. *Biochem Cell Biol*, 93: 102-7.
- Mann A, Miksys S, Lee A, Mash DC, Tyndale RF. (2008). Induction of the drug metabolizing enzyme CYP2D in monkey brain by chronic nicotine treatment. *Neuropharmacology*, 55: 1147-55.
- McMillan DM, Tyndale RF. (2015). Nicotine Increases Codeine Analgesia Through the Induction of Brain CYP2D and Central Activation of Codeine to Morphine. *Neuropsychopharmacology*, 40: 1804-12.
- McMillan DM, Tyndale RF. (2017). Inducing rat brain CYP2D with nicotine increases the rate of codeine tolerance; predicting the rate of tolerance from acute analgesic response. *Biochem Pharmacol*, 145: 158-68.
- McMillan DM, Tyndale RF. (2018). CYP-mediated drug metabolism in the brain impacts drug response. *Pharmacol Ther*, 184: 189-200.
- Miksys S, Rao Y, Sellers EM, Kwan M, Mendis D, Tyndale RF. (2000). Regional and cellular distribution of CYP2D subfamily members in rat brain. *Xenobiotica*, 30: 547-64.
- Miksys S, Wadji FB, Tolledo EC, Remington G, Nobrega JN, Tyndale RF. (2017). Rat brain CYP2D enzymatic metabolism alters acute and chronic haloperidol side-effects by different mechanisms. *Prog Neuropsychopharmacol Biol Psychiatry*, 78: 140-8.
- Miksys SL, Tyndale RF. (2002). Drug-metabolizing cytochrome P450s in the brain. *J Psychiatry Neurosci*, 27: 406-15.

- Mizuno D, Hiroi T, Ng P, Kishimoto W, Imaoka S, Funae Y. (2003). Regulation of CYP2D expression in rat brain by toluene. *Osaka City Med J*, 49: 49-56.
- Navarro-Mabarak C, Camacho-Carranza R, Espinosa-Aguirre JJ. (2018). Cytochrome P450 in the central nervous system as a therapeutic target in neurodegenerative diseases. *Drug Metab Rev*: 1-14.
- Penas-Lledo EM, Llerena A. (2014). CYP2D6 variation, behaviour and psychopathology: implications for pharmacogenomics-guided clinical trials. *Br J Clin Pharmacol*, 77: 673-83.
- Sangar MC, Anandatheerthavarada HK, Tang W, Prabu SK, Martin MV, Dostalek M, Guengerich FP, Avadhani NG. (2009). Human liver mitochondrial cytochrome P450 2D6--individual variations and implications in drug metabolism. *FEBS J*, 276: 3440-53.
- Toselli F, Dodd PR, Gillam EM. (2016). Emerging roles for brain drug-metabolizing cytochrome P450 enzymes in neuropsychiatric conditions and responses to drugs. *Drug Metab Rev*, 48: 379-404.
- Tyndale RF, Li Y, Li NY, Messina E, Miksys S, Sellers EM. (1999). Characterization of cytochrome P-450 2D1 activity in rat brain: high-affinity kinetics for dextromethorphan. *Drug Metab Dispos*, 27: 924-30.
- Voirol P, Jonzier-Perey M, Porchet F, Reymond MJ, Janzer RC, Bouras C, Strobel HW, Kosel M, Eap CB, Baumann P. (2000). Cytochrome P-450 activities in human and rat brain microsomes. *Brain Res*, 855: 235-43.
- Wan J, Imaoka S, Chow T, Hiroi T, Yabusaki Y, Funae Y. (1997). Expression of four rat CYP2D isoforms in *Saccharomyces cerevisiae* and their catalytic specificity. *Arch Biochem Biophys*, 348: 383-90.

- Wang Q, Han X, Li J, Gao X, Wang Y, Liu M, Dong G, Yue J. (2015). Regulation of cerebral CYP2D alters tramadol metabolism in the brain: interactions of tramadol with propranolol and nicotine. *Xenobiotica*, 45: 335-44.
- Wang X, Li J, Dong G, Yue J. (2014). The endogenous substrates of brain CYP2D. *Eur J Pharmacol*, 724: 211-8.
- Wattiaux-De Coninck S, Dubois F, Wattiaux R. (1974). Effect of imipramine on the behavior of rat-liver mitochondria during centrifugation in a sucrose gradient. *Eur J Biochem*, 48: 407-16.
- Wu JY, Yue J, Feng YQ. (2011). Determination of brain cytochrome P450 2E1 activity in rat with the probe of chlorzoxazone by liquid chromatography-mass spectrometry. *J Chromatogr B Analyt Technol Biomed Life Sci*, 879: 260-6.
- Wyss A, Gustafsson JA, Warner M. (1995). Cytochromes P450 of the 2D subfamily in rat brain. *Mol Pharmacol*, 47: 1148-55.
- Yue J, Miksys S, Hoffmann E, Tyndale RF. (2008). Chronic nicotine treatment induces rat CYP2D in the brain but not in the liver: an investigation of induction and time course. *J Psychiatry Neurosci*, 33: 54-63.
- Zhou K, Khokhar JY, Zhao B, Tyndale RF. (2013). First demonstration that brain CYP2D-mediated opiate metabolic activation alters analgesia in vivo. *Biochem Pharmacol*, 85: 1848-55.

LEGENDS TO FIGURES

Figure 1. Dextromethorphan O-demethylase activity as a function of substrate concentration in the rat brain microsomes, crude mitochondria, and purified mitochondria (A) and in the whole homogenate and total membranes (B). Incubations were carried out at 37°C with 0.2 mg/mL protein for 20 minutes. Symbols and error bars represent the average and SD of the experimental data, respectively ($n = 5$). The lines represent the best fit to the data based on a single-enzyme, MM model (A) or two-enzyme, mixed model (B).

Figure 2. Estimated dextromethorphan-O-demethylation kinetic parameters of rat brain microsomes (MC), crude mitochondria (CM), and purified mitochondria (PM). A single-enzyme, MM model was used to estimate apparent maximum velocity (V_{\max}) (A), MM constant (K_m) (B), and intrinsic clearance (CL_{int}) (C). The symbols and horizontal lines represent individual and average data, respectively ($n = 5$). Statistical analyses were performed with repeated measures, one-way ANOVA, followed by Tukey's post-hoc test. *, $p < 0.05$; **, $p < 0.01$; and ***, $p < 0.001$.

Figure 3. Estimated dextromethorphan-O-demethylation kinetic parameters of rat brain total membranes (TM) and whole homogenates (WH). A two-enzyme, mixed model was used to estimate apparent maximum velocity ($V_{\max 1}$) (A), MM constant (K_{m1}) (B), and intrinsic clearance ($CL_{\text{int}1}$) (C) for the first enzyme and $CL_{\text{int}2}$ (D) for the second enzyme. The symbols and horizontal lines represent individual and average data, respectively ($n = 5$). Statistical analyses were performed with an unpaired, two-tailed t-test. ****, $p < 0.0001$.

Figure 4. Immunoblot analysis of CYP2D (A), VDAC (B), and calreticulin (C) in microsomes (MC), purified mitochondria (PM), crude mitochondria (CM), and total membranes (TM) fractions in rat brains. For each panel, densitometry data for individual samples (left) and representative blots (right) are presented. For each protein, the densitometry data are presented as the percentage

of the highest abundant fraction. The symbols and horizontal lines in the left panels represent individual and average data, respectively ($n = 5$). Statistical analyses were performed with repeated measure, one-way ANOVA, followed by Tukey's post-hoc test. A p value of < 0.05 was considered significant. Means with the same letter are significantly different from each other.

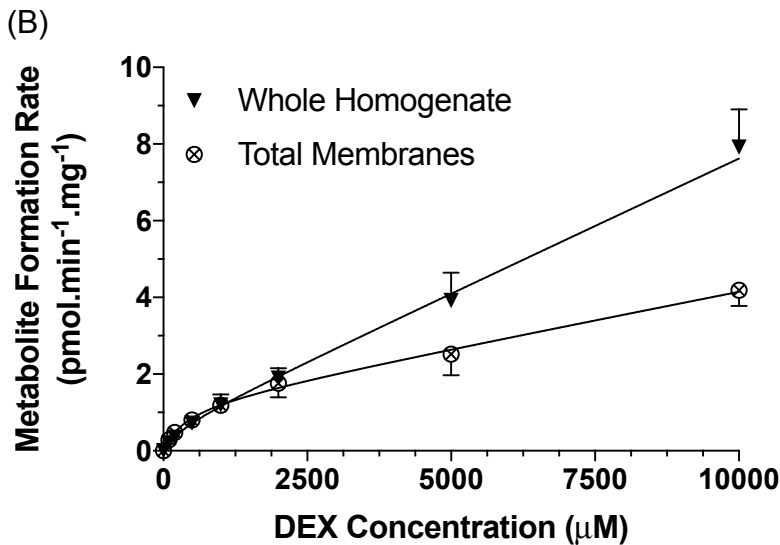
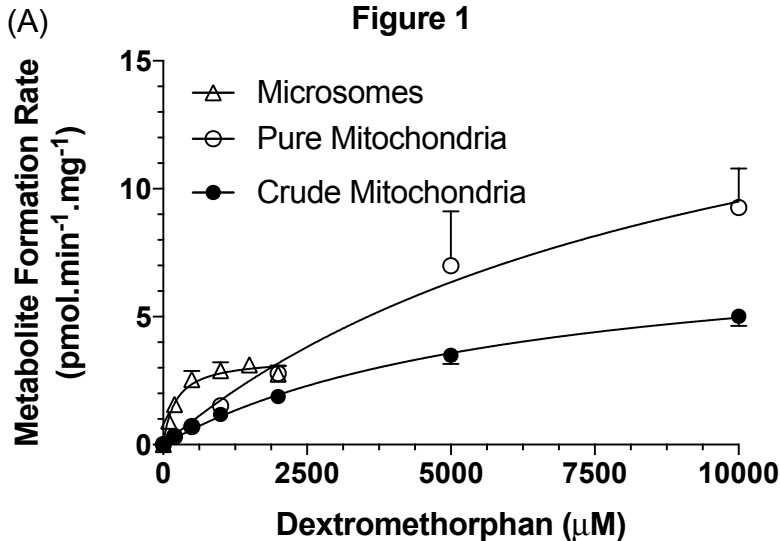
Figure 1

Figure 2

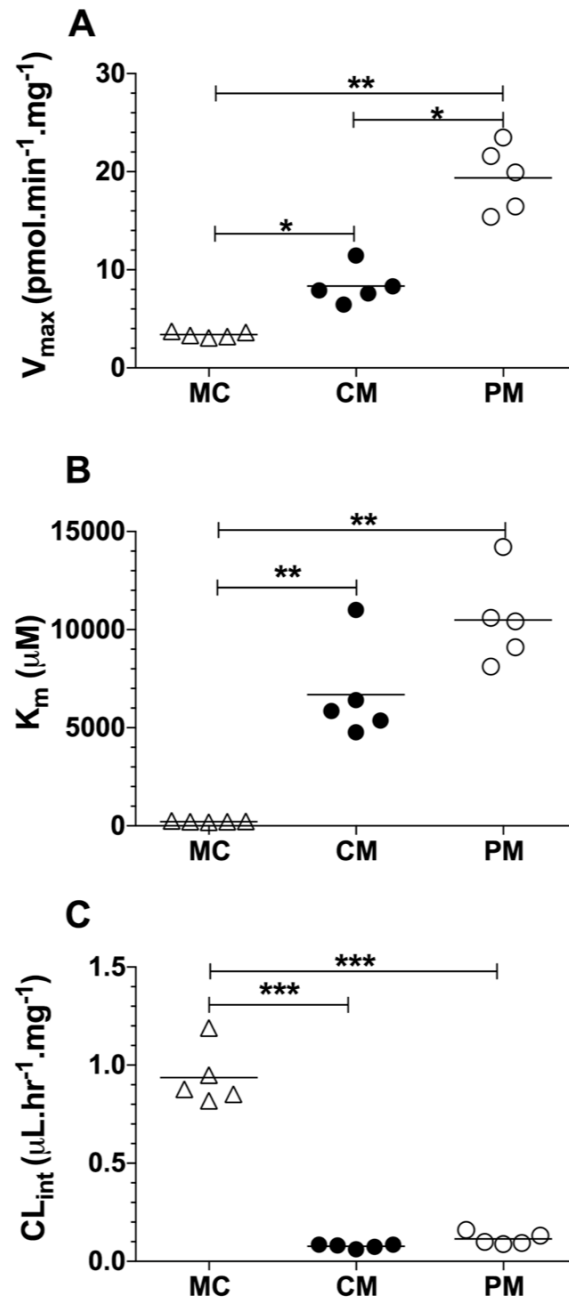


Figure 3

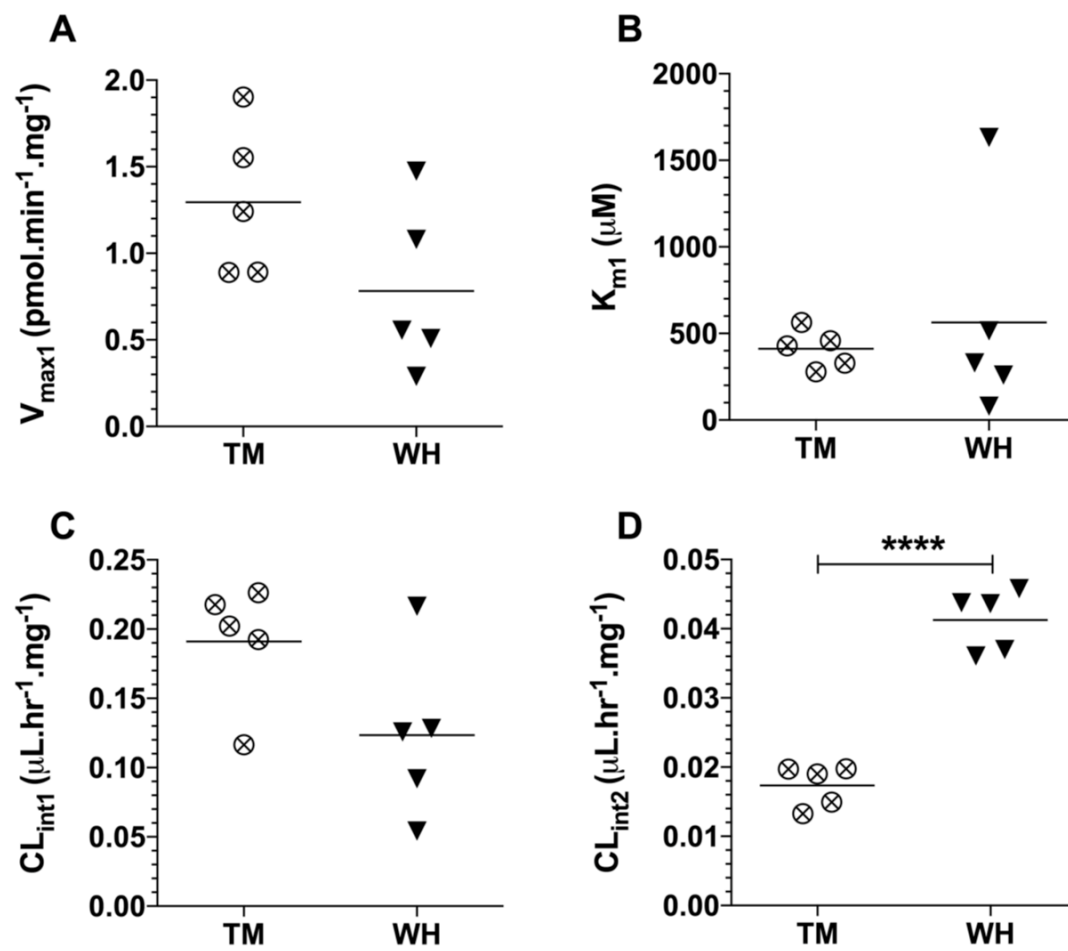
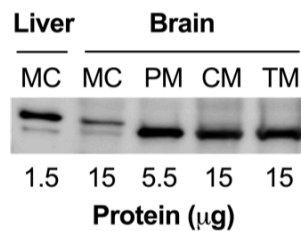
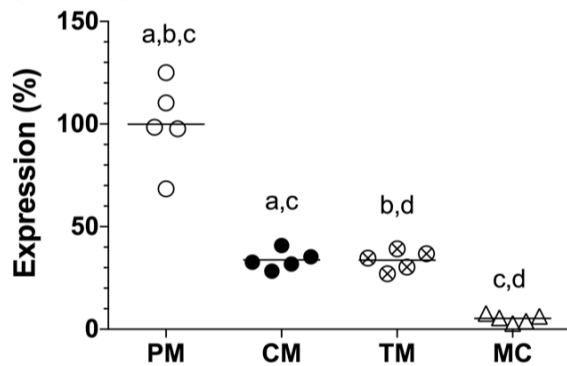
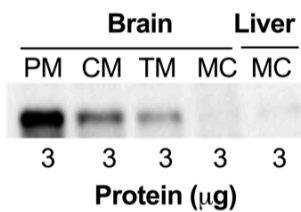
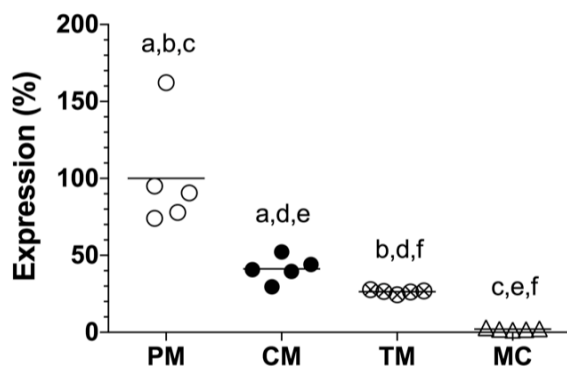


Figure 4

A (CYP2D)



B (VDAC)



C (Calreticulin)

